Materials Research Proceedings 41 (2024) 2262-2270 https://doi.org/10.21741/9781644903131-249

A strategy for minimizing the computational time of simulations involving near-surface embossing of sheet metal materials

HEINZELMANN Pascal[1,a*], GÖRZ Marcel[1,b], RIEDMÜLLER Kim Rouven[1,c] and LIEWALD Mathias[1, d]

[1]Institute for Metal Forming Technology, University of Stuttgart,

Holzgartenstraße 17, 70174 Stuttgart, Germany

[a] pascal.heinzelmann; [b]marcel.goerz; [c]kim.riedmueller; [d]mathias.liewald}@ifu.uni-stuttgart.de

Keywords: Embossing, Dual-Phase Steel, Simulation, Mapping

Abstract. By near-surface embossing, work hardening can be introduced into sheet metal blanks, thus increasing the material´s yield strength. Hence, this property-modifying process can be used to improve the lightweight potential of a component on the one hand and its crash performance on the other. For the early design of such embossing or forming processes and to predict the modification of the material properties, FE modelling is currently used. Here, the embossing of the near-surface structures is usually simulated first, followed by the forming process. However, existing simulation methods are time-consuming and computationally intensive, due to the simulation of the whole embossing process. For this purpose, this paper presents two approaches for improving the simulation time of embossing and forming processes. Compared to the conventional holistic embossing and forming simulation, these approaches are based on a new mapping strategy and experimental data. In the mapping variant, solid elements' stress and strain distribution is mapped to shell elements, thus including the embossing history for the forming simulation. For the experimental-based variant, the yield curves of embossed tensile tests are determined and used to approximate the property changes in the simulation. Both concepts are compared with each other and the conventional simulation method in terms of accuracy and calculation time. This paper finally shows that simulation can be performed faster with the new approaches than with the current sequential modelled workflow.

Introduction

Human-induced climate change is caused primarily by the emission of greenhouse gases such as CO_2, which is largely produced by motorised traffic. Therefore, both the US, the EU, and other countries have made commitments to significantly reduce these emissions, particularly from road transport [1]. In addition to filtering and storing such gases as they are emitted, another promising measure being driven by the automotive industry is the general reduction of fossil fuel consumption. Here, lightweight design approaches such as the use of lightweight aluminium alloys or tailoring mechanical material properties in critical areas of sheet metal components provide a promising contributions [2].

The selective modification of material properties in highly loaded areas of sheet metal components allows comparatively thin sheet metal materials to be used in manufacturing and thus to reduce weight of such components. In particular, the selective application of near-surface embossing can induce strain hardening in relevant areas of the component, which can lead to an improvement in mechanical properties [3]. Initial tests on this topic were carried out by Namoco et al. in 2006 on work-hardened aluminium alloys A6061-T4 and A5052-H34 [4]. Further, Abel et al. demonstrated the improved formability of embossed deep-drawn components made of aluminium sheets [5]. Studies with DP steels conducted by Walzer et al. revealed an increase in the tensile strength of the dual-phase (DP) steel DP600 due to near-surface embossing [6].

Additionally, three-point bending tests with embossed DP500 of Briesenick et al. showed an increase in the maximum bending force [7]. Complementary to the work of Walzer and Briesenick, tensile tests and three-point bending tests with higher-strength DP800 were conducted by Heinzelmann et al., yielding comparable results [8, 9].

However, the aforementioned studies also showed that introducing embossing as part of the development process of sheet metal components poses a challenge. This is mainly due to the fact that there is still no standardized workflow for developing embossed sheet metal components. When designing embossed components, additional embossing simulations must be conducted before the conventional metal forming simulation. To perform such simulations, solid elements are recommended to accurately represent the influences of embossing on the sheet metal structure and properties. Thus, use of solid element formulation allows the complex stress states introduced by near-surface embossing to be accurately modelled. This is of crucial importance as these stresses play a major role in the development process and associated simulations. [8]. To use the results of the embossing simulations for subsequent forming simulations, these also have to be performed with solid elements. This leads to two disadvantages: Firstly, the calculation of solid element simulations requires more computational time than equivalent shell element simulations. Secondly, solvers for the simulation of sheet metal components are optimised to calculate with shell elements only [10].

One approach to overcome this problem is to transfer the results of the simulation with solid element mesh to a shell element mesh [11]. When mapping from a solid mesh to a shell mesh, the stresses and strains of the solid elements are transcribed to the integration points of the corresponding shell elements. This allows the results of embossing simulations to be transferred to the shell elements of a forming simulation. However, this approach still involves a solid element simulation for the embossing. To further reduce the calculation time, the embossing simulation therefore needs to be further optimised. The maximum reduction would occur if only the forming simulation is necessary without a prior embossing simulation. Therefore, this paper presents a new approach that avoids the need for prior embossing simulations. This approach simulates the embossed areas with different material properties than the rest of the component. This means that the embossing simulation can be completely avoided and the computation time for the development of embossed components is reduced. This approach assumes that

- the introduced changes in mechanical properties are homogeneously distributed over the embossing area and that the material properties depend on the embossing pattern,
- the geometry of the final component is not affected by the embossing, and
- the transition between embossed and unembossed component areas can be discretised, i.e. neighbouring elements can have different material properties.

Method

In this paper, three simulation workflows are compared regarding their computational time for forming process with embossed sheet metal materials. The first approach represents the current state-of-the-art for designing near-surface embossed parts. Here, a forming simulation is preceded by an embossing simulation which adds the results (stresses, strains, and sheet-metal thickness) of the embossing to the initial sheet material of the forming simulation before it starts. This requires both the embossing simulation and the process simulation to be performed with solid elements. The approach will therefore be referred to as the “solid approach”. The second approach also includes a preceded embossing simulation, but its results are mapped to a shell mesh. This mapped mesh is used for the forming simulation without further modification. Therefore, the forming simulation does not have to be carried out with solid elements but can retain shell element formulation. Further on, this approach will be mentioned as “mapping approach”. To further improve computational efficiency, the paper describes a final approach that eliminates the need

for prior embossing simulation. Here, the embossed areas are characterised solely by specific material properties in the modelling of the sheet metal material for the forming simulation. The material properties of the embossed areas differ from the rest of the part. This approach will be referred to as the "material approach".

The comparison of the aforementioned approaches was carried out using two common practical examples, the tensile test and the three-point bending test. The tensile test thereby represented the "ideal" uniaxial stress state. The three-point bending test was used to investigate a more complex stress state. Both tests were performed simulatively and experimentally. To quantify the influence of the embossing, the tests were performed with specimens having different embossing patterns. All embossings were applied in a regular hexagonal pattern, which is defined by the embossing distance *a* (distance from one embossing to the respective neighbouring embossings) and the depth of the embossings. For the study carried out, distances *a* of 1.0 mm, 1.5 mm and 2.0 mm were investigated. Each pattern was applied to the sheet material with two embossing depths t_{emb} (depth of penetration of the embossing punch measured from the surface to be embossed) of 100 µm and 200 µm (see Figure 1). This resulted in six different embossing patterns. For the tests, the dual-

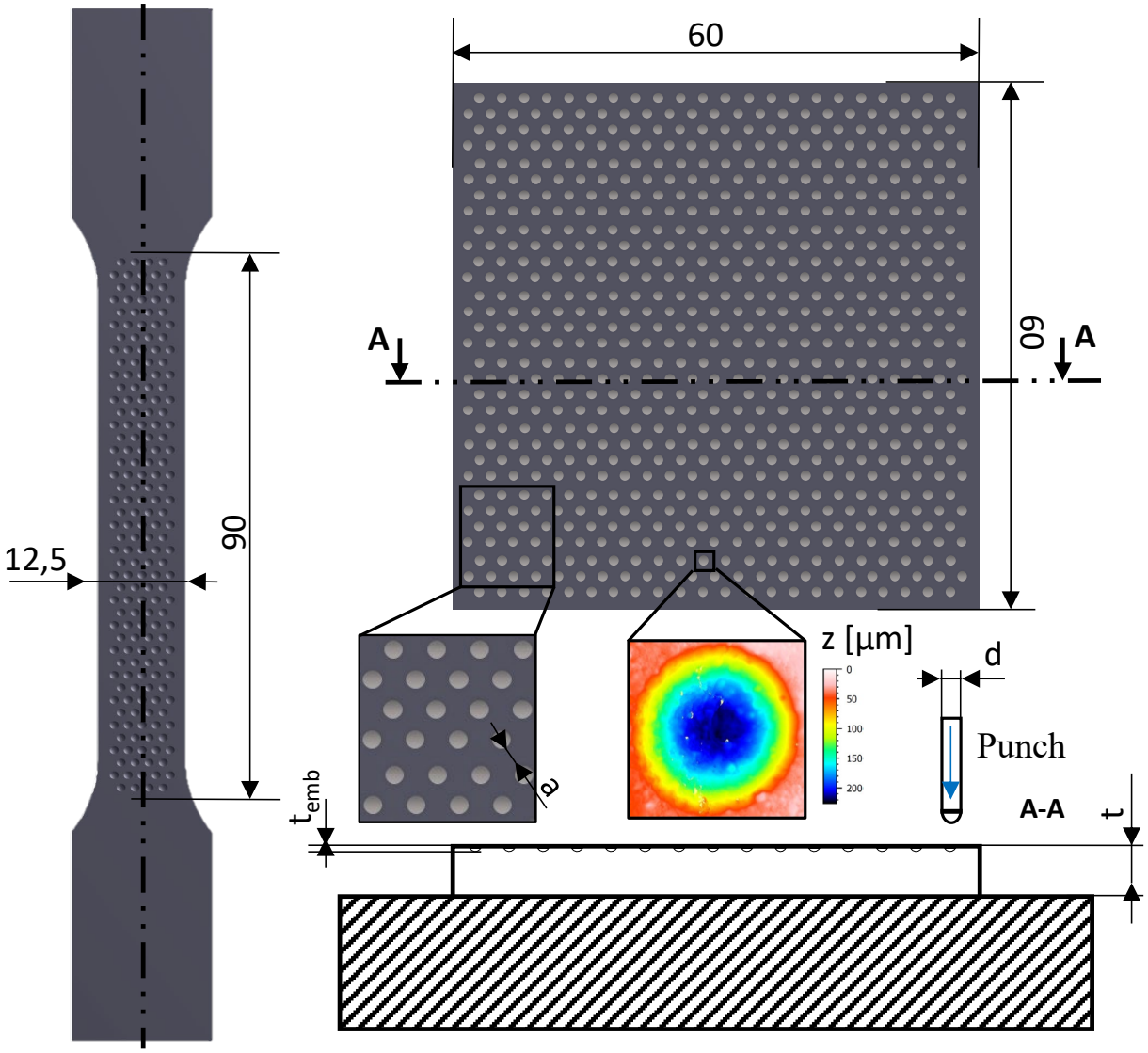

Figure 1: General overview of the embossed specimens with representation of the dimensions and the variables.

phase (DP) steel DP800 with a sheet thickness of 1.5 mm, which is commonly used in the automotive industry, was considered.

Test specimens for the real experiments were produced with a Trumpf TRUPunch 5000R CNC punching machine. This machine is capable of up to 1.400 strokes per minute. A round punch with a diameter *d* of 4 mm and the front surface milled into a hemisphere was used to apply the embossing patterns. For the tensile specimens, the embossing patterns were first applied onto a sheet metal blank, from which the final geometry was milled afterwards in accordance with DIN 50125-H20×80 [12]. The specimens for the three-point bending tests were first embossed and then punched to 60 x 60 mm. The tensile and three-point bending tests were performed on a Roell + Korthaus RKM100 universal testing machine. The tensile tests were carried out according to DIN EN ISO 6892-1 [13] and the three-point bending tests according to DIN EN ISO 7438 [14]. During all tests, the force and displacement curves were recorded (see Figure 2).

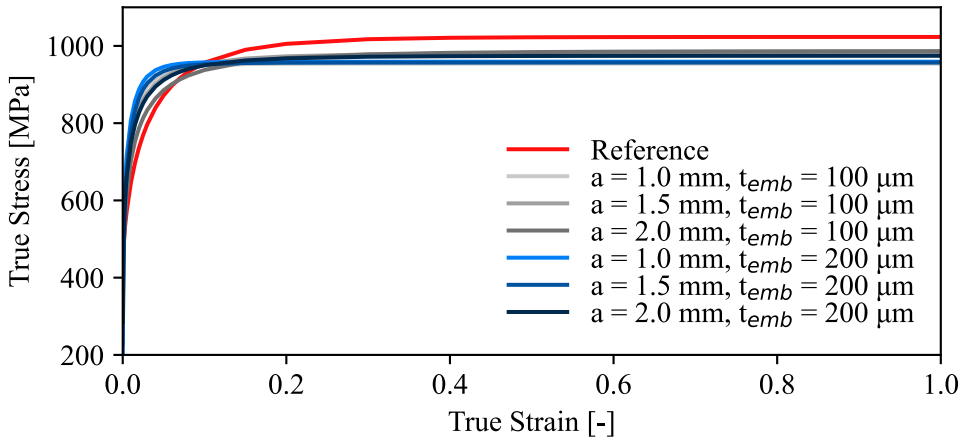

Figure 2: Extrapolated flow curves of the six embossing patterns and the unembossed reference.

For simulating the tests according to the real counterpart, the LS-DYNA solver was used. All simulations were performed using the material model "*MAT_024", as it represents the material sufficiently accurately. The flow curves used to describe the hardening behaviour are shown in Figure 2. The flow curves were included in the simulation as tabular data. The simulations were performed on an Intel® Core™ i7-7700 processor (8 cores @ 3.6 GHz). The simulation models of all approaches consisted of three parts: embossing punch (rigid), die (rigid) and specimen. The rigid parts were modelled using shell elements. As a representation of the punch, a spherical segment and for the die a plane surface was chosen. The edges' nodes of the specimen were fixed translationally and rotationally in all spatial dimensions. The movement of the punch and die was synchronised for embossing in the x and y direction. Further, in the z direction, these parts moved opposingly. Depending on the embossing pattern, the embossing punch penetrated the specimen 100 µm respectively 200 µm. The contact formulation "*CONTACT_ONE_WAY_SURFACE_TO_SURFACE_FORMING" was used to model the contact between the specimen and the tool surfaces. For the solid approach, the specimen geometry was meshed using solid elements with an element edge length of 0.5 mm. The results of the embossing simulations were written as a "dynain" file and subsequently used for the forming simulations. For the shell approach, the specimen's geometry was meshed with shell elements. The results of the solid approach's embossing simulation were mapped to the shell mesh of the forming simulation using the mapping software Envyo®. For the material approach, an additional embossing simulation was not required. The material model was changed globally for the experiments regarding this paper. However, for each embossing pattern, a new material card had

to be created for the forming simulation in order to match the specific material properties. Since the material model "*MAT_024" can be described with only a flow curve, the experimental data of the embossed tensile tests were used to generate the custom material cards. The flow curves were created using the stress-strain values of the tensile tests. As these values are only valid up to the yield point, the curves were extrapolated for higher degrees of deformation [15]. The extrapolation was performed according to the Hockett-Sherby method [16]. The flow curves respectively the material cards were generated for the unembossed material and the six embossing patterns (see Figure 2). The simulations were set up according to DIN EN ISO 6892-1 for the tensile tests and DIN EN ISO 7438 for the three-point bending tests. Like the experiments, the force and displacement curves were calculated in the simulation as well. The force in the tensile test was determined using a cross-section plane. It was placed in the centre of the specimen to calculate the force of the middle elements. For the three-point bending test, the force was given by the reaction force between the bending punch and the specimen. The displacements in both tests were determined by the node displacement.

Results

To compare the approaches, the computation time required for the simulations was used as a benchmark. Figure 3 shows the average calculation time for the three approaches. All tensile test simulations, including the various embossing patterns and the reference test, were utilized. This figure shows the average calculation times of the different embossing patterns.

The mapping approach is 15.8 %, and the material approach is 90.5 % faster than the solid approach. When comparing the mapping approach with the material approach, the material approach is 87.5 % faster than the mapping approach. This clearly shows how large a part of the total calculation time is due to the embossing simulation and how great the advantages of the material approach are compared to the approaches with a prior embossing simulation.

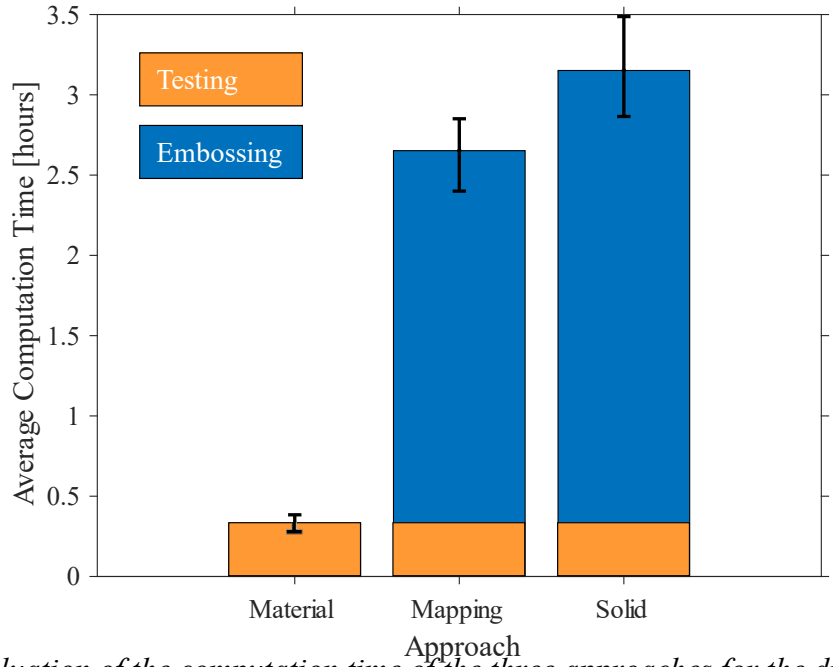

Figure 3: Evaluation of the computation time of the three approaches for the different embossing geometries and the tensile tests.

The assessment of the different approaches was based on force-displacement curves derived from three-point bending tests. Figure 4 illustrates these curves, which include both experimental data and results from the solid, mapping and material approaches for a specific parameter set

(h = 100 µm, a = 2 µm). The qualitative evaluation involved comparing how well each approach agreed with the observed experimental results. Initially, simulations of the three-point bending test were set up for the unembossed case using both solid and shell elements. Apart from the use of different elements, the simulations did not differ. These simulations were then adapted for the embossed specimens and hasn't been fitted to the reality, so the computational times were comparable. As a result, there are deviations to the experiment. It's worth noting that the embossing process, which takes place before the test, induces deformation in the specimen. Consequently, the deformed specimens do not rest fully on the supports. The sub-figures in Figure 4 show the differences in the specimens, with the solid approach (upper left) taking this deformation into account, whereas the mapping and material approaches (upper right) do not. As a result, the curves of the experiment and the solid approach show good similarities in the early stages, as both the mapping and material approaches were simulated with a flat, undeformed shell mesh, while the solid approach used a deformed solid mesh. In contrast, the two shell approaches (mapping and material approach) start with full contact, skipping the initial deformation required to achieve full contact with the supports and bending punch. Additionally, challenges associated with the embossing process were identified but not considered in the simulation, including slight variations in embossing depth, changes in geometry after embossing, and interactions of the embossings. Reproducing these proved challenging and time-consuming, particularly when using a simple material model. Furthermore, the bending punch and the support is considered rigid, and the stiffness of the universal testing machine and tools used were not considered, which may not accurately represent real-world conditions, as a universal testing machine is not perfectly rigid.

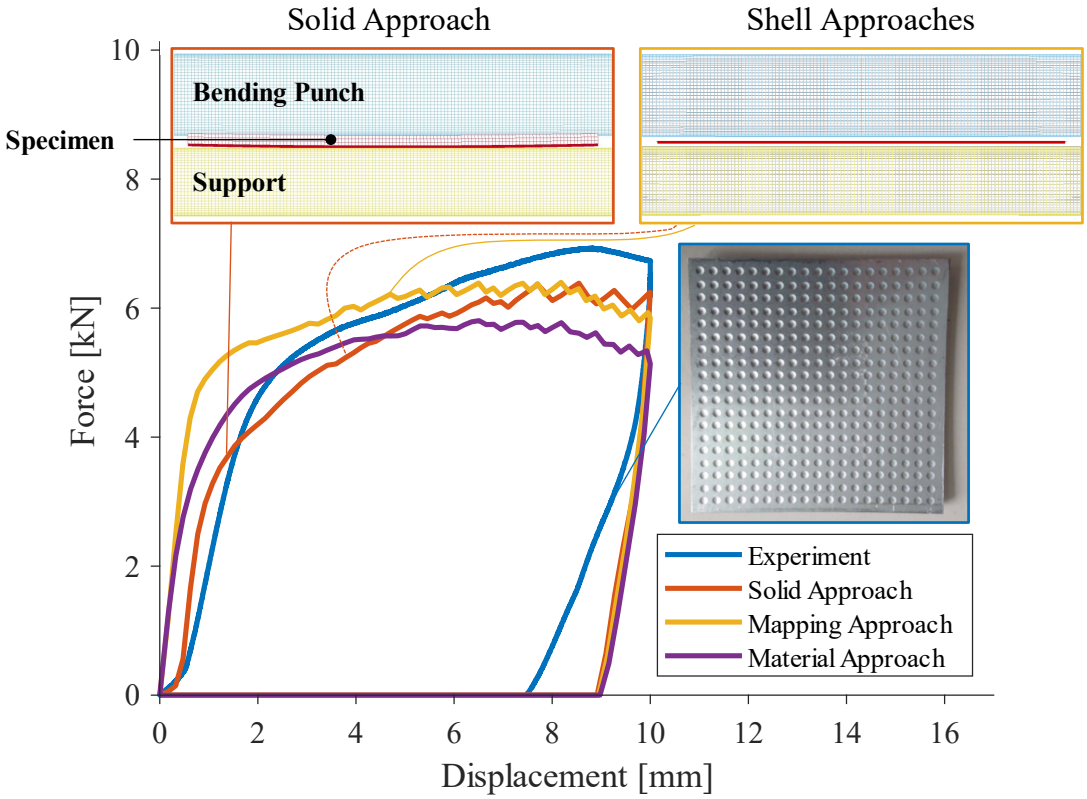

Figure 4: Example (h = 100 µm, a = 2 mm) of the force displacement curves of the experiment, solid approach, mapping approach, and material approach.

Conclusion and Outlook

In this paper, two new approaches for the forming simulation of embossed components were considered for and compared with the conventional simulation method with regard to the required computing time. For the conventional solid approach, both the embossing simulation and the process simulations were considered. For the mapping approach, the results of an embossing simulation with solid elements (solid approach) were mapped to the integration points of the forming simulations' shell mesh. Since the additional computation time of the process simulation is only due to the preceding embossing simulation, the last material approach attempted to dispense the embossing simulation by approximating embossed areas by selectively adjusting the material properties in the forming simulation. This required different material cards for the embossed and unembossed areas.

In order to compare the approaches with each other, two different material tests were carried out both simulatively and experimentally with selectively embossed specimens. Here, tensile tests according to DIN EN ISO 6892-1 and three-point bending tests according to DIN EN ISO 7438 were performed. A total of six embossing patterns were investigated, varying in embossing distance (1 mm, 1.5 mm, and 2 mm) and depth (100 µm and 200 µm). As no additional embossing simulation was required, the calculation time for the material approach revealed as the shortest. The other two approaches each include a preceding solid embossing simulation, which makes them significantly slower. As the solid approach also involves adapting the forming simulation to a solid representation of the specimen and an additional embossing simulation, this approach is the slowest. To minimise this aspect, the mapping approach was proposed, where the results of the solid simulation were mapped to the integration points of the shell elements of the forming simulation. This led to a reduction of the computation time, but was far from achieving the short calculation time of the material approach. To compare the approaches, only the computation time was considered in this paper. The preparation and adaptation of the simulations, the mapping from solid to shell elements, and the creation of the material cards were not considered in terms of time in any way. Difficulties in quantifying the individual preparation steps are the reason for this. Qualitatively, all approaches were able to reproduce the experiments well. At the start of the force-displacement curve, the solid approach was able to reproduce the initial setting of the specimen better than the other two approaches due to the additional change in geometry introduced by the embossing. The course of the experiment is also slightly better represented by the solid approach.

The approaches presented here to model embossed areas offers enormous potential for speeding up the design and development of embossed sheet metal components. The fundamental advantages have been described and quantified for the first time in this paper. Simple tests with simple stress states have been considered. Whether this approach is also suitable for more complex design methods used in industrial practice remains to be verified. The simulations considered here were also carried out with a simple material model. For more complex examples, it will also be necessary to adapt this model. This will also result in more complex material characterization tests to be carried out on embossed and unembossed materials. If for more complex cases it is found that the approximation with the material approach is not sufficiently fast or accurate, it would also be conceivable to adapt the mapping approach. For example, this approach could be used to simulate a single embossing with solid elements and the results could be copied and mapped into the corresponding embossing pattern.

Acknowledgements

The research project "Herstellung crashoptimierter Blechbauteile mittels Prägen" of the Europäische Forschungsvereinigung EFB e. V. is carried out in the framework of the industrial collective research programme (IGF no. 21940N). It is supported by the Federal Ministry for Economic Affairs and Climate Action (BMWK) through the AiF (German Federation of Industrial Research Associations e. V) based on a decision taken by the German Bundestag. Additionally,

we would like to thank our project partners DYNAmore GmbH, Eckold GmbH & Co. KG, synchropress GmbH, Engineering System International GmbH, Karosseriewerke Dresden GmbH, Zeller + Gmelin GmbH & Co. KG, Novelis Switzerland SA, Tata Steel Europe, STRACK NORMA GmbH & Co. KG, F+K Werkstoffprüfung und Labor GmbH, and KIRCHHOFF Automotive GmbH.

References

[1] K. Shanmugam, V. Gadhamshetty, P. Yadav, D. Athanassiadis, M. Tysklind, and V. K. Upadhyayula, "Advanced High-Strength Steel and Carbon Fiber Reinforced Polymer Composite Body in White for Passenger Cars: Environmental Performance and Sustainable Return on Investment under Different Propulsion Modes," *ACS Sustainable Chem. Eng.*, vol. 7, no. 5, pp. 4951–4963, 2019. https://doi.org/10.1021/acssuschemeng.8b05588

[2] H. E. Friedrich, *Leichtbau in der Fahrzeugtechnik*. Wiesbaden: Springer Fachmedien Wiesbaden, 2017.

[3] C. S. Namoco, T. Iizuka, R. C. Sagrado, N. Takakura, and K. Yamaguchi, "Experimental and numerical investigation of restoration behavior of sheet metals subjected to bulging deformation," *Journal of Materials Processing Technology*, vol. 177, 1-3, pp. 368–372, 2006. https://doi.org/10.1016/j.jmatprotec.2006.03.208

[4] C. S. Namoco, T. Iizuka, K. Narita, N. Takakura, and K. Yamaguchi, "Effects of embossing and restoration process on the deep drawability of aluminum alloy sheets," *Journal of Materials Processing Technology*, vol. 187-188, pp. 202–206, 2007. https://doi.org/10.1016/j.jmatprotec.2006.11.182

[5] Y. Abe, K. Mori, T. Maeno, S. Ishihara, and Y. Kato, "Improvement of sheet metal formability by local work-hardening with punch indentation," *Prod. Eng. Res. Devel.*, vol. 13, no. 5, pp. 589–597, 2019. https://doi.org/10.1007/s11740-019-00910-6

[6] S. Walzer, M. Liewald, N. Simon, J. Gibmeier, H. Erdle, and T. Böhlke, "Improvement of Sheet Metal Properties by Inducing Residual Stresses into Sheet Metal Components by Embossing and Reforming," *Applied Science and Engineering Progress*, vol. 15, no. 1, 2021. https://doi.org/10.14416/j.asep.2021.09.006

[7] D. Briesenick, S. Walzer, and M. Liewald, "Study on the Effect of Embossing on the Bending Properties of High-Strength Sheet Metals," in *Forming the Future: Proceedings of the 13th International Conference on the Technology of Plasticity* (The Minerals, Metals & Materials Series), G. Daehn, J. Cao, B. Kinsey, E. Tekkaya, A. Vivek, and Y. Yoshida, Eds., 1st ed. Cham: Springer International Publishing; Imprint Springer, 2021, pp. 2585–2595

[8] P. Heinzelmann, D. Briesenick, and M. Liewald, "Characterization of the Mechanical Properties of Selectively Embossed Sheet Metal Materials Under Multi-Axial Loads," *IOP Conf. Ser.: Mater. Sci. Eng.*, vol. 1284, no. 1, p. 12043, 2023. https://doi.org/10.1088/1757-899X/1284/1/012043

[9] P. Heinzelmannn, D. Briesenick, and M. Liewald, "Modifying mechanical properties of sheet metal materials by work hardening mechanisms induced by selective embossing," in *Material Forming*, Lukasz Madej, Mateusz Sitko, Konrad Perzynski, Ed., 2023, pp. 951–958. https://doi.org/10.21741/9781644902479-104

[10] E. Madenci, *The Finite Element Method and Applications in Engineering Using ANSYS®,* 2nd ed. (SpringerLink Bücher). Boston, MA: Springer, 2015.

[11] C. Liebold and A. Haufe, “process2product simulation: Closing Incompatibilities in Constitutive Modeling and Spatial Discretization with envyo®,” in Dearborn, Michigan, USA, 2018.

[12] *Prüfung metallischer Werkstoffe – Zugproben*, DIN 50125, DIN Deutsches Institut für Normung e. V., Berlin, 2022.

[13] *Metallische Werkstoffe - Zugversuch: Teil 1: Prüfverfahren bei Raumtemperatur (ISO 6892-1:2019)*, DIN EN ISO 6892-1, DIN Deutsches Institut für Normung e. V., Berlin, 2020.

[14] *Metallische Werkstoffe - Biegeversuch (ISO 7438:2020)*, DIN EN ISO 7438, DIN Deutsches Institut für Normung e. V., Berlin, 2021.

[15] A. R. Birkert, S. Haage, and M. Straub, *Umformtechnische Herstellung komplexer Karosserieteile: Auslegung von Ziehanlagen*. Berlin, Heidelberg: Springer Vieweg, 2013.

[16] J. E. Hockett and O. D. Sherby, “Large strain deformation of polycrystalline metals at low homologous temperatures,” *Journal of the Mechanics and Physics of Solids*, vol. 23, no. 2, pp. 87–98, 1975. https://doi.org/10.1016/0022-5096(75)90018-6